Real-Time Simulation of Large Open Quantum Spin Systems driven by Measurements

D. Banerjee[1], F.-J. Jiang[2], M. Kon[3], and U.-J. Wiese[1]
[1] *Albert Einstein Center, Institute for Theoretical Physics, Bern University, 3012 Bern, Switzerland*
[2] *Department of Physics, National Taiwan Normal University 88, Sec. 4, Ting-Chou Rd., Taipei 116, Taiwan*
[3] *Department of Mathematics, Boston University, Boston, Massachusetts, U.S.A.*

We consider a large quantum system with spins $\frac{1}{2}$ whose dynamics is driven entirely by measurements of the total spin of spin pairs. This gives rise to a dissipative coupling to the environment. When one averages over the measurement results, the corresponding real-time path integral does not suffer from a sign problem. Using an efficient cluster algorithm, we study the real-time evolution of a 2-d Heisenberg antiferromagnet, which is driven to a disordered phase, either by sporadic measurements or by continuous monitoring described by Lindblad evolution.

arXiv:1405.7882v1 [cond-mat.str-el] 30 May 2014

Simulating the real-time evolution of large quantum systems is a notoriously hard problem. On the one hand, due to the enormous dimension of the Hilbert space, which grows exponentially with the system size, diagonalizing the Hamiltonian is impossible in practice. On the other hand, the configurations contributing to the real-time path integral have complex weights, which prevents the application of the Monte Carlo method based on importance sampling. While this method often works extremely well for Euclidean time simulations of quantum systems in thermal equilibrium, it fails for real-time simulations, due to a severe sign or complex weight problem. A notable exception are gapped 1-d systems with small entanglement, for which the matrix product states underlying the density matrix renormalization group [1, 2] provide a good basis for simulating the real-time evolution, at least for moderate time intervals [3–9]. Also Euclidean time simulations may suffer from severe sign problems, for example, in fermionic systems away from half-filling or in the presence of frustrating interactions. Some sign problems even fall in the complexity class of NP-complete problems [10], which can be solved in polynomial time on a hypothetical "non-deterministic" computer, but not on an ordinary deterministic computer (unless NP would unexpectedly coincide with the complexity class P). This means that a general method for solving sign problems is unlikely to exist, and that these problems should thus be addressed on a case by case basis. In fact, several severe sign problems have been solved completely using the meron-cluster algorithm [11, 12] or the fermion bag approach [13–15].

It is not surprising that classical computers have problems simulating quantum systems, in particular, in real time. The entanglement inherent in complex quantum phases is not easily representable, let alone computable, as classical information. For this reason, as early as 1982 Feynman proposed using specifically designed quantum devices to mimic quantum systems that are difficult to simulate classically [16]. Since the ground-breaking experimental realization of Bose-Einstein condensation [17, 18], the fields of atomic physics and quantum optics have undergone impressive development. The degree to which ultracold atomic systems can be engineered and controlled is truly remarkable, and Feynman's vision of quantum simulators is becoming a reality. For example, the bosonic Hubbard model has been implemented with exquisitely well-controlled ultracold atoms in an optical lattice [19], and several aspects of this quantum simulation have been verified by comparison with accurate quantum Monte Carlo simulations [20]. Digital [21] and analog [22] quantum simulators are widely discussed in atomic and condensed matter physics [23–28], and more recently also in a particle physics context [29–37].

While quantum simulators are gradually becoming available, they are far from being universally applicable, and they are not yet precision instruments. Hence, simulating the real-time evolution of large quantum systems on classical computers remains an important challenge. Since isolated quantum systems tend to evolve into complicated entangled states such as those of Schrödinger's cat, it will in general be extremely difficult to compute them classically. In the real world, Schrödinger cat states usually do not arise, because quantum systems suffer from decoherence by coupling to their environment, and thus behave more classically. It should hence be easier to simulate quantum systems in the presence of an environment. Here we develop a method to simulate the real-time evolution of large quantum spin systems whose dynamics are entirely driven by measurements of the total spin $(\vec{S}_x + \vec{S}_y)^2$ of pairs of spins $\frac{1}{2}$ at adjacent positions x and y. The measurements give rise to a dissipative coupling to the environment, which drives the system from an initial state to a new equilibrium. Remarkably, when one averages over the measurement results, the sign problem is eliminated and the dynamics can be addressed with an efficient cluster algorithm. This is the first time that the real-time evolution of a large strongly coupled quantum system can be simulated over arbitrarily long time intervals in any spatial dimension. The dissipative measurement process that drives the time-evolution may even be realizable in optical lattice experiments. The control of quantum systems by measurements is investigated in [38, 39], and dynamical phenomena in out-of-equilibrium quantum systems are

discussed in [40–50]. Measurements have also been suggested as a resource for quantum computation [51–54]. In non-relativistic quantum mechanics, the path integral representation of measurement processes has been discussed in [55, 56].

Let us consider a general quantum system with a (possibly time-dependent) Hamiltonian, whose real-time evolution from t_k to t_{k+1} is described by the time-evolution operator $U(t_{k+1},t_k) = U(t_k,t_{k+1})^\dagger$. At time t_k ($k \in \{1,2,\ldots,N\}$) we assume an observable O_k is measured and an eigenvalue o_k is obtained as the measurement result. The Hermitean operator P_{o_k} projects on the subspace of the Hilbert space spanned by the eigenvectors of O_k with eigenvalue o_k. Starting from an initial density matrix $\rho_0 = \sum_i p_i |i\rangle\langle i|$ (with $0 \le p_i \le 1$, $\sum_i p_i = 1$) at time t_0, the probability of reaching a final state $|f\rangle$ at time t_f, after a sequence of N measurements with results o_k, is then given by [57]

$$\begin{aligned} &p_{\rho_0 f}(o_1,o_2,\ldots,o_N) = \\ &\sum_i \langle i|U(t_0,t_1)P_{o_1}U(t_1,t_2)P_{o_2}\ldots P_{o_N}U(t_N,t_f)|f\rangle \\ &\langle f|U(t_f,t_N)P_{o_N}\ldots P_{o_2}U(t_2,t_1)P_{o_1}U(t_1,t_0)|i\rangle p_i. \end{aligned} \quad (1)$$

The matrix elements of both the time-evolution and the projection operators are in general complex, thus leading to a severe sign problem in Monte Carlo simulations. As we have argued above, classical measurements disentangle the quantum system, at least to some extent, and should thus alleviate the sign problem. For simplicity, we now consider quantum systems whose time-evolution is entirely driven by measurements, i.e. $U(t_k,t_{k+1}) = \mathbb{1}$. By inserting complete sets of states $\sum_{n_k} |n_k\rangle\langle n_k| = \mathbb{1}$ into the first factor and independently $\sum_{n'_k} |n'_k\rangle\langle n'_k| = \mathbb{1}$ into the second factor in eq. (1), between the times t_k, one arrives at a real-time path integral along the Keldysh contour leading from t_0 to t_f and back [58, 59]. In the doubled Hilbert space of states $|n_k n'_k\rangle$, encompassing both pieces of the Keldysh contour,

$$\begin{aligned} &p_{\rho_0 f}(o_1,o_2,\ldots,o_N) = \\ &\sum_i p_i \langle ii|(P_{o_1}\otimes P^*_{o_1})(P_{o_2}\otimes P^*_{o_2})\ldots(P_{o_N}\otimes P^*_{o_N})|ff\rangle = \\ &\sum_i p_i \sum_{n_1,n'_1}\cdots\sum_{n_{N-1},n'_{N-1}} \prod_{k=1}^{N} \langle n_{k-1}n'_{k-1}|P_{o_k}\otimes P^*_{o_k}|n_k n'_k\rangle. \end{aligned} \quad (2)$$

We use the notation $\langle n_{k-1}n'_{k-1}|P_{o_k}\otimes P^*_{o_k}|n_k n'_k\rangle = \langle n_{k-1}|P_{o_k}|n_k\rangle\langle n'_{k-1}|P_{o_k}|n'_k\rangle^*$, $\langle n_0 n'_0| = \langle ii|$, and $|n_N n'_N\rangle = |ff\rangle$. We also consider the probability $p_{\rho_0 f}$ of reaching the final state $|f\rangle$ irrespective of the intermediate measurement results,

$$\begin{aligned} p_{\rho_0 f} &= \sum_{o_1}\sum_{o_2}\cdots\sum_{o_N} p_{\rho_0 f}(o_1,o_2,\ldots,o_N) \\ &= \sum_i p_i \sum_{n_1,n'_1}\cdots\sum_{n_{N-1},n'_{N-1}} \prod_{k=1}^{N} \langle n_{k-1}n'_{k-1}|\widetilde{P}_k|n_k n'_k\rangle, \end{aligned} \quad (3)$$

where $\widetilde{P}_k = \sum_{o_k} P_{o_k}\otimes P^*_{o_k}$ is obtained by summing over all possible measurement results o_k at time t_k.

Besides the process of sporadic measurements, let us also consider quantum systems that are continuously monitored by their environment. This situation is characterized by a set of Lindblad operators [60, 61] $L_{o_k} = \sqrt{\varepsilon\gamma}P_{o_k}$ (related to Kraus operators [62]) that obey $(1-\varepsilon\gamma N)\mathbb{1} + \sum_{k,o_k} L^\dagger_{o_k}L_{o_k} = \mathbb{1}$. Here γ determines the probability of measurements per unit time, and $k \in \{1,2,\ldots,N\}$ labels the operators O_k (with eigenvalues o_k) that can induce quantum jumps at any moment in time. In the continuous time limit, $\varepsilon \to 0$, and in the absence of a Hamiltonian, the time-evolution of the density matrix is then determined by the Lindblad equation

$$\begin{aligned} \partial_t\rho &= \frac{1}{\varepsilon}\sum_{k,o_k}\left(L_{o_k}\rho L^\dagger_{o_k} - \frac{1}{2}L^\dagger_{o_k}L_{o_k}\rho - \frac{1}{2}\rho L^\dagger_{o_k}L_{o_k}\right) \\ &= \gamma\sum_k\Big(\sum_{o_k} P_{o_k}\rho P_{o_k} - \rho\Big). \end{aligned} \quad (4)$$

As a simple example, let us first consider two spins $\frac{1}{2}$, $\vec{S}_x$ and $\vec{S}_y$, forming total spin S eigenstates $|SS^3\rangle$ (with 3-component S^3): $|11\rangle = \uparrow\uparrow$, $|10\rangle = \frac{1}{\sqrt{2}}(\uparrow\downarrow + \downarrow\uparrow)$, $|1-1\rangle = \downarrow\downarrow$, and $|00\rangle = \frac{1}{\sqrt{2}}(\uparrow\downarrow - \downarrow\uparrow)$. The projection operators corresponding to a measurement 1 or 0 of the total spin are then given by $P_1 = |11\rangle\langle 11| + |10\rangle\langle 10| + |1-1\rangle\langle 1-1|$ and $P_0 = |00\rangle\langle 00|$, such that

$$P_1 = \begin{pmatrix} 1 & 0 & 0 & 0 \\ 0 & \frac{1}{2} & \frac{1}{2} & 0 \\ 0 & \frac{1}{2} & \frac{1}{2} & 0 \\ 0 & 0 & 0 & 1 \end{pmatrix}, \quad P_0 = \begin{pmatrix} 0 & 0 & 0 & 0 \\ 0 & \frac{1}{2} & -\frac{1}{2} & 0 \\ 0 & -\frac{1}{2} & \frac{1}{2} & 0 \\ 0 & 0 & 0 & 0 \end{pmatrix}. \quad (5)$$

The negative entries in P_0 give rise to a sign problem in the corresponding real-time path integral. We quantize the spins in the 3-direction, with $s_x = \pm\frac{1}{2}$ denoting the eigenvalues of S^3_x. In the doubled Hilbert space of states $|n_k n'_k\rangle = |s_{x,k}s_{y,k}s'_{x,k}s'_{y,k}\rangle$ one then obtains

$$\begin{aligned} &\langle s_{x,k}s_{y,k}s'_{x,k}s'_{y,k}|\widetilde{P}|s_{x,k+1}s_{y,k+1}s'_{x,k+1}s'_{y,k+1}\rangle = \\ &(\delta_{s_{x,k},s_{x,k+1}}\delta_{s_{y,k},s_{y,k+1}}\delta_{s'_{x,k},s'_{x,k+1}}\delta_{s'_{y,k},s'_{y,k+1}} \\ &+\delta_{s_{x,k},s_{y,k+1}}\delta_{s_{y,k},s_{x,k+1}}\delta_{s'_{x,k},s'_{y,k+1}}\delta_{s'_{y,k},s'_{x,k+1}})/2. \end{aligned} \quad (6)$$

All matrix elements of $\widetilde{P} = P_1\otimes P_1^* + P_0\otimes P_0^*$ are non-negative. The Kronecker δ-functions encode loop-cluster rules for binding parallel spins together [63, 64]. The Lindblad process is the continuous-time limit of the discrete measurement process, which can be simulated directly in continuous time [65]. Remarkably, the resulting cluster algorithm allows very efficient real-time simulations, without encountering a sign problem.

The simple two-spin system is easily extended to a large system in any dimension. We investigate a system of quantum spins $\frac{1}{2}$ on a square lattice of size $L\times L$ with periodic boundary conditions. To define an initial density matrix $\rho_0 = \exp(-\beta H)$, we consider the antiferromagnetic Heisenberg Hamiltonian, $H = J\sum_{\langle xy\rangle}\vec{S}_x\cdot\vec{S}_y$,

which is used only to prepare an ensemble of initial states, not to evolve it further in time. The real-time evolution is again driven entirely by the measurement of the total spin $(\vec{S}_x + \vec{S}_y)^2$ of nearest-neighbor spin pairs. In a first step, all pairs of neighboring spins separated in the 1-direction, at $x = (x_1, x_2)$ and $y = (x_1 + 1, x_2)$ with even x_1, are measured simultaneously. In a second step, the pairs at (x_1, x_2) and (x_1, x_2+1) with even x_2, which are separated in the 2-direction, are examined. In a third and fourth measurement step, the total spins of pairs with odd x_1 and x_2 are being measured. Then the same four-step measurement process is repeated an arbitrary number of times M, such that the total number of measurements is $N = 4M$. This particular measurement sequence was chosen arbitrarily and can be replaced by any other one. For the Lindblad process the ordering of the measurements is irrelevant. Together with the Keldysh contour, the Euclidean time interval $[0, \beta]$ (where $T = 1/\beta$ is the temperature) forms a closed contour in the complex time plane. The clusters, which are closed loops extending through both real and Euclidean time, are updated by simultaneously flipping all spins belonging to the same cluster with probability $\frac{1}{2}$. Remarkably, as a global consequence of eq. (6), the clusters, and thus also the spin configurations that contribute to the real-time path integral, are identical on both parts of the Keldysh contour, i.e. $s_{x,k} = s'_{x,k}$. Then eq. (6) simplifies to

$$\begin{aligned}&\langle s_{x,k} s_{y,k} s_{x,k} s_{y,k} | \widetilde{P} | s_{x,k+1} s_{y,k+1} s_{x,k+1} s_{y,k+1} \rangle = \\ &(\delta_{s_{x,k}, s_{x,k+1}} \delta_{s_{y,k}, s_{y,k+1}} + \delta_{s_{x,k}, s_{y,k+1}} \delta_{s_{y,k}, s_{x,k+1}})/2 = \\ &\langle s_{x,k} s_{y,k} | P_1 | s_{x,k+1} s_{y,k+1} \rangle. \end{aligned} \tag{7}$$

We have investigated the real-time evolution of initial state ensembles corresponding to the 2-d square lattice Heisenberg antiferromagnet. While the uniform magnetization, $\vec{M} = \sum_x \vec{S}_x$, i.e. the total spin, is conserved in the measurement process, the staggered magnetization, $M_s = \sum_x (-1)^{x_1 + x_2} S^3_x$, as well as the other Fourier modes $\widetilde{S}(p) = \sum_x S^3_x \exp(ip_1 x_1 + ip_2 x_2)$, $p = (p_1, p_2)$, are affected by the measurements. Fig. 1a shows the staggered magnetization squared, averaged over the ensemble of final states $|f\rangle$ that results after N discrete measurements, for systems with different initial temperatures. They are quickly driven to a new equilibrium ensemble.

In order to study the equilibration process in more detail, we now consider continuous Lindblad evolution, from an initial ensemble at low temperature $\beta J = 5L/2a$, where a is the lattice spacing. Fig. 1c shows the real-time evolution of the Fourier modes

$$\langle |\widetilde{S}(p)|^2 \rangle \to A(p) + B(p) \exp(-t/\tau(p)), \tag{8}$$

for a variety of momenta $p = (p_1, p_2)$. While the conserved magnetization $\vec{M}$ with momentum $p = (0, 0)$ does not equilibrate at all, low momentum modes equilibrate more slowly than high momentum modes. After a short

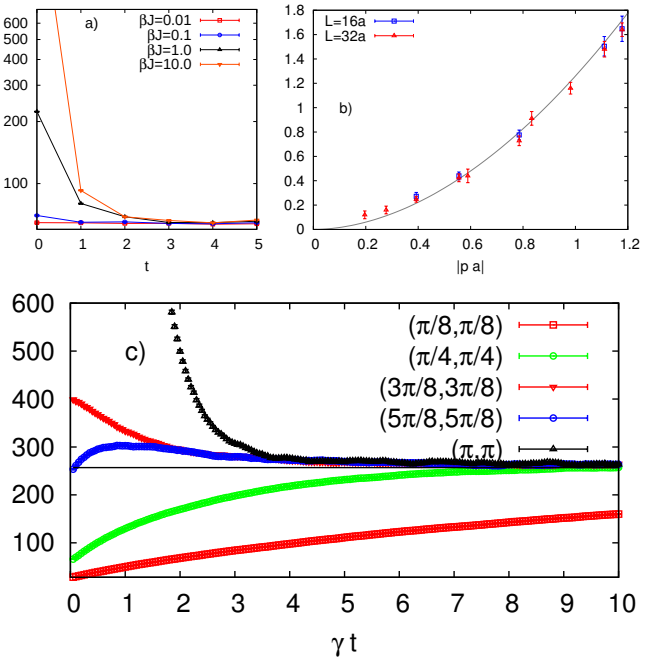

FIG. 1. [Color online] *a) Real-time evolution of* $\langle M_s^2 \rangle$ *driven by discrete measurements, for* $\beta J = 0.01$, 0.1, 1, *and* 10, *for* $L = 16a$. *b) Inverse equilibration time* $1/[\gamma\tau(p)]$ *as a function of* $|p|$ *for* $L = 16a$, $\beta J = 40$, *and* $L = 32a$, $\beta J = 80$. *c) Evolution of the Fourier modes* $\langle |\widetilde{S}(p)|^2 \rangle$ *for the Heisenberg antiferromagnet driven by a continuous Lindblad process.*

initial phase, the various modes approach the ultimate new equilibrium exponentially, with an equilibration time $\tau(p)$. Interestingly, for fixed momentum, $\tau(p)$ is almost independent of the spatial volume. Large systems equilibrate slowly, because they contain modes of low momentum. For small momenta, the equilibration time behaves as $1/[\gamma\tau(p)] = C|pa|^r$, $C = 1.26(8)$, $r = 1.9(2)$ (Fig. 1b).

Since the measurement process conserves the total spin $\vec{S} = \sum_x \vec{S}_x$, it does not change the probability distribution of the spin associated with the initial density matrix ρ_0. The continuous-time Lindblad process even respects the translation and rotation symmetries of the lattice. The final density matrix, to which the system is driven by the measurements, is constrained by these symmetries, and is proportional to the unit matrix in each symmetry sector. This finally leads to a vanishing correlation length and to $A(p) = L^4/4(L^2-1)$, indicated by the horizontal line in Fig. 1c. The unit density matrix (restricted to the appropriate symmetry sectors) is a stable $T = \infty$ fixed point of any Hamiltonian plus Lindbladian dynamics, and thus a universal attractor for the ultimate long-term evolution for a large class of dissipative processes.

For the initial density matrix ρ_0 of the antiferromagnet, $\langle M_s^2 \rangle / L^2$ is proportional to L^2, indicating spontaneous symmetry breaking of the $SU(2)$ spin symmetry at zero temperature. By the Lindblad process the system is driven to a final density matrix for which $\langle M_s^2 \rangle / L^2$

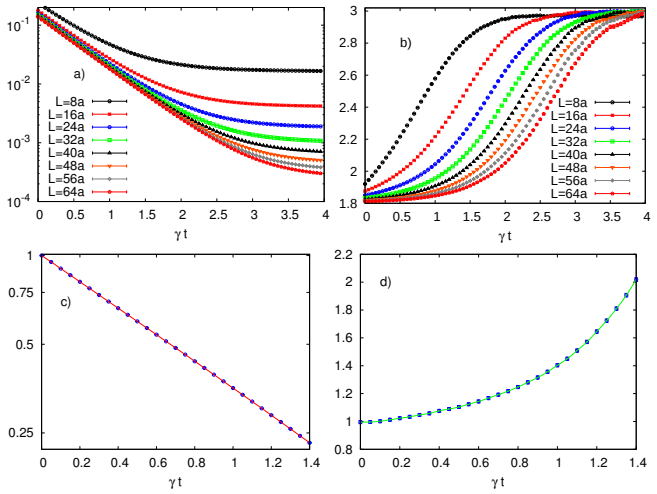

FIG. 2. [Color online] *a)* $\langle M_s^2\rangle/L^4$ *and b) Binder ratio* $\langle M_s^4\rangle/\langle M_s^2\rangle^2$ *as functions of time for* $L/a = 12, \ldots, 48$, $\beta J = 8, \ldots, 30$. *Evolution of c)* $\mathcal{M}_s(t)/\mathcal{M}_s(0)$ *and d)* $\xi(t)/\xi(0)$.

becomes volume-independent, indicating that the $SU(2)$ spin symmetry is then restored. Consequently, the system must undergo a phase transition. Since the dissipative Lindblad process drives the system far out of thermal equilibrium, this phase transition is not expected to fall to any of the standard dynamical universality classes [66]. Figs. 2a,b show $\langle M_s^2\rangle/L^4$ and the Binder ratio $\langle M_s^4\rangle/\langle M_s^2\rangle^2$ for $\beta J = 2L/3a$. The various finite-volume curves for the Binder ratio do not intersect. Instead, with increasing volume their inflection point moves to later times. Figs. 2c,d show the staggered magnetization density $\mathcal{M}_s$ and the length scale $\xi = c/(2\pi\rho_s)$, where c is the spinwave velocity and ρ_s is the spin stiffness, as functions of time, obtained by a fit to

$$\langle M_s(t)^2\rangle = \frac{\mathcal{M}_s(t)^2 L^4}{3} \sum_{n=0}^{3} c_n \left(\frac{\xi(t)}{L}\right)^n, \qquad (9)$$

which implicitly defines $\mathcal{M}_s(t)$ and $\xi(t)$. Here the constants $c_0 = 1$, $c_1 = 5.7503(6)$, $c_2 = 16.31(2)$, $c_3 = -84.8(2)$ (which are accurately determined at $t = 0$) are assumed to be time-independent. The order parameter $\mathcal{M}_s(t) = \mathcal{M}_s(0)\exp(-t/\tau)$ (with $\mathcal{M}_s(0) = 0.30743(1)/a^2$ [67, 68]) decays exponentially with $\gamma\tau = 0.240(2)$, which suggests that the phase transition is completed only after an infinite amount of time. The length scale $\xi(t)$ (with $\xi(0) = 1.459(3)a$ [68]) increases with time, which can be attributed to a decrease of ρ_s.

By averaging over all measurement results, we have eliminated the sign problem. When one distinguishes individual measurement results, one encounters a sign problem. When one measures spin $S = 1$, one obtains

$$\langle s_{x,k}s_{y,k}s'_{x,k}s'_{y,k}|P_1 \otimes P_1^*|s_{x,k+1}s_{y,k+1}s'_{x,k+1}s'_{y,k+1}\rangle =$$
$$(\delta_{s_{x,k},s_{x,k+1}}\delta_{s_{y,k},s_{y,k+1}}\delta_{s'_{x,k},s'_{x,k+1}}\delta_{s'_{y,k},s'_{y,k+1}}$$
$$+\delta_{s_{x,k},s_{y,k+1}}\delta_{s_{y,k},s_{x,k+1}}\delta_{s'_{x,k},s'_{x,k+1}}\delta_{s'_{y,k},s'_{y,k+1}}$$
$$+\delta_{s_{x,k},s_{x,k+1}}\delta_{s_{y,k},s_{y,k+1}}\delta_{s'_{x,k},s'_{y,k+1}}\delta_{s'_{y,k},s'_{x,k+1}}$$
$$+\delta_{s_{x,k},s_{y,k+1}}\delta_{s_{y,k},s_{x,k+1}}\delta_{s'_{x,k},s'_{y,k+1}}\delta_{s'_{y,k},s'_{x,k+1}})/4, \qquad (10)$$

which is always non-negative. Again, the Kronecker δ-functions encode rules for forming clusters of parallel spins. The four contributions to the right-hand side of eq. (10) correspond to four different cluster break-ups of the eight contributing spins. When we measure the total spin $S = 0$, we obtain

$$\langle s_{x,k}s_{y,k}s'_{x,k}s'_{y,k}|P_0 \otimes P_0^*|s_{x,k+1}s_{y,k+1}s'_{x,k+1}s'_{y,k+1}\rangle =$$
$$(s_{x,k}-s_{y,k})(s_{x,k+1}-s_{y,k+1})(s'_{x,k}-s'_{y,k})(s'_{x,k+1}-s'_{y,k+1})/4$$
$$\times\delta_{s_{x,k},-s_{y,k}}\delta_{s_{x,k+1},-s_{y,k+1}}\delta_{s'_{x,k},-s'_{y,k}}\delta_{s'_{x,k+1},-s'_{y,k+1}}, \qquad (11)$$

which may indeed be negative. In this case, the Kronecker δ-functions assign anti-parallel spins on neighboring spatial sites to the same cluster. Interestingly, the resulting sign problem is similar to the one that arises for geometrically frustrated quantum antiferromagnets in Euclidean time, which has been addressed with a nested cluster algorithm in [69]. While this algorithm reduces the sign problem by a factor that is exponential in the space-time volume, in general it does not solve the problem completely. If we distinguish only a few measurement results, and average over the other ones, the sign problem remains manageable, and can be solved by the nested cluster algorithm.

We have considered quantum spin systems whose real-time evolution is entirely driven by measurements of the total spin of spin pairs. Remarkably, when one averages over the measurement results, the corresponding real-time path integral is unaffected by the sign problem and has been simulated with a very efficient loop-cluster algorithm. Subsequent measurements at discrete times as well as a related dissipative continuous-time Lindblad process destroy long-range antiferromagnetic correlations of the initial density matrix, and drive the system to a new equilibrium with only short-range correlations. Our method can be applied to other initial density matrices and can be extended to other measurement processes that drive the real-time evolution. It will be interesting to investigate the real-time evolution of a variety of initial states by various dissipative measurement processes, which may even by realizable in optical lattice experiments with ultracold atoms. A challenging next step will be to combine measurements with the real-time evolution driven by a non-trivial Hamiltonian.

We like to thank J. Berges, S. Chandrasekharan, F. Niedermayer and P. Zoller for illuminating discussions. MK and UJW thank the CTP at MIT, where this work was initiated, for hospitality during a sabbatical. UJW is grateful to J. Fröhlich for stimulating discussions a long time ago. The research leading to these results has received funding from the Schweizerischer Nationalfonds and from the European Research Council under

the European Union's Seventh Framework Programme (FP7/2007-2013)/ ERC grant agreement 339220.

[1] S. R. White, Phys. Rev. Lett. 68 (1992) 2863.
[2] U. Schollwöck, Rev. Mod. Phys. 77 (2005) 259.
[3] G. Vidal, Phys. Rev. Lett. 91 (2003) 147902.
[4] S. R. White and A. E. Feiguin, Phys. Rev. Lett. 93 (2004) 076401.
[5] F. Verstraete, I. I. Garcia-Ripoll, and J. I. Cirac, Phys. Rev. Lett. 93 (2004) 207204.
[6] M. Zwolak and G. Vidal, Phys. Rev. Lett. 93 (2004) 207205.
[7] A. J. Daley, C. Kollath, U. Schollwöck, and G. Vidal, J. Stat. Mech.: Theor. Exp. P04005 (2004).
[8] T. Barthel, U. Schollwöck, and S. R. White, Phys. Rev. B79 (2009) 245101.
[9] I. Pizorn, V. Eisler, S. Andergassen, and M. Troyer, arXiv:1305.0504.
[10] M. Troyer and U.-J. Wiese, Phys. Rev. Lett. 94 (2005) 170201.
[11] W. Bietenholz, A. Pochinsky, and U.-J. Wiese, Phys. Rev. Lett. 75 (1995) 4524.
[12] S. Chandrasekharan and U.-J. Wiese, Phys. Rev. Lett. 83 (1999) 3116.
[13] S. Chandrasekharan, Phys. Rev. D82 (2010) 025007.
[14] S. Chandrasekharan and A. Li, Phys. Rev. Lett. 108 (2012) 140404.
[15] E. F. Huffman and S. Chandrasekharan, Phys. Rev. B89 (2014) 111101.
[16] R. P. Feynman, Int. J. Theor. Phys. 21 (1982) 467.
[17] M. H. Anderson, J. R. Ensher, M. R. Matthews, C. E. Wieman, and E. A. Cornell, Science 269 (1995) 5221.
[18] K. B. Davis, M. O. Mewes, M. R. Andrews, N. J. van Druten, D. S. Durfee, D. M. Kurn, and W. Ketterle, Phys. Rev. Lett. 75 (1995) 3969.
[19] M. Greiner, O. Mandel, T. Esslinger, T. W. Hänsch, and I. Bloch, Nature 415 (2002) 39.
[20] S. Trotzky, L. Pollet, F. Gerbier, U. Schnorrberger, I. Bloch, N. Prokovéf, B. Svistunov, and M. Troyer, Nature Phys. 6 (2010) 998.
[21] S. Lloyd, Science 273 (1996) 1073.
[22] D. Jaksch, C. Bruder, J. I. Cirac, C. W. Gardiner, and P. Zoller, Phys. Rev. Lett. 81 (1998) 3108.
[23] J. I. Cirac and P. Zoller, Nature Phys. 8 (2012) 264.
[24] M. Lewenstein, A. Sanpera, and V. Ahufinger, "Ultracold Atoms in Optical Lattices: Simulating Quantum Many-Body Systems", Oxford University Press (2012).
[25] I. Bloch, J. Dalibard, and S. Nascimbene, Nature Phys. 8 (2012) 267.
[26] R. Blatt and C. F. Ross, Nature Phys. 8 (2012) 277.
[27] A. Aspuru-Guzik, P. Walther, Nature Phys. 8 (2012) 285
[28] A. A. Houck, H. E. Türeci, and J. Koch, Nature Phys. 8 (2012) 292.
[29] E. Kapit, E. Mueller, Phys. Rev. A83 (2011) 033625.
[30] G. Szirmai, E. Szirmai, A. Zamora, and M. Lewenstein, Phys. Rev. A84 (2011) 011611.
[31] E. Zohar, J. Cirac, and B. Reznik, Phys. Rev. Lett. 109 (2012) 125302.
[32] D. Banerjee, M. Dalmote, M. Müller, E. Rico, P. Stebler, U.-J. Wiese, and P. Zoller, Phys. Rev. Lett. 109 (2012) 175302.
[33] D. Banerjee, M. Bögli, M. Dalmote, E. Rico, P. Stebler, U.-J. Wiese, and P. Zoller, Phys. Rev. Lett. 110 (2013) 125303.
[34] E. Zohar, J. Cirac, and B. Reznik, Phys. Rev. Lett. 110 (2013) 125304.
[35] L. Tagliacozzo, A. Celi, P. Orland, M. W. Mitchell, and M. Lewenstein, Nature Commun. 4 (2013) 2615.
[36] L. Tagliacozzo, A. Celi, A. Zamora, and M. Lewenstein, Ann. Phys. 330 (2013) 160.
[37] U.-J. Wiese, Annalen der Physik 525 (2013) 777.
[38] M. Sugawara, J. Chem. Phys. 123 (2005) 204115.
[39] A. Pechen, N. Il'in, F. Shuang, and H. Rabitz, Phys. Rev. A74 (2006) 052102.
[40] J. M. Cornwall, R. Jackiw, and E. Tomboulis, Phys. Rev. D (1974) 2428.
[41] J. Berges, Nucl. Phys. A699 (2002) 847.
[42] G. Aarts, D. Ahrensmeier, R. Baier, J. Berges, and J. Serreau, Phys. Rev. D66 (2002) 045008.
[43] J. Berges, A. Rothkopf, and J. Schmidt, Phys. Rev. Lett. 101 (2008) 041603.
[44] S. Diehl, A. Micheli, A. Kantian, B. Kraus, H. P. Büchler, and P. Zoller, Nature Phys. 4 (2008) 878.
[45] E. G. Dalla Torre, E. Demler, T. Giamarchi, and E. Altman, Nature Phys. 6 (2009) 806.
[46] F. Verstraete, M. M. Wolf, and J. I. Cirac, Nature Phys. 5 (2009) 633.
[47] S. Diehl, A. Tomadin, A. Micheli, R. Fazio, and P. Zoller, Phys. Rev. Lett. 105 (2010) 015702.
[48] M. Müller, S. Diehl, G. Pupillo, and P. Zoller, Adv. Atom. Mol. Opt. Phys. 61 (2012) 1.
[49] L. M. Sieberer, S. D. Huber, E. Altman, and S. Diehl, Phys. Rev. Lett. 110 (2013) 195301.
[50] C. De Grandi, A. Polkovnikov, and A. W. Sandvik, J. Phys.: Cond. Matt. 25 (2013) 404216.
[51] R. Raussendorf and H. J. Briegel, Phys. Rev. Lett. 86 (2001) 5188.
[52] M. A. Nielsen, Phys. Lett. A308 (2003) 96.
[53] A. M. Childs, E. Deotto, E. Farhi, J. Goldstone, S. Gutmann, and A. J. Landahl, Phys. Rev. A66 (2002) 032314.
[54] P. Aliferis and D. W. Leung, Phys. Rev. A70 (2004) 062314.
[55] M. B. Mensky, Phys. Rev. D20 (1979) 384.
[56] C. M. Caves, Phys. Rev. D33 (1986) 1643.
[57] R. B. Griffiths, J. Stat. Phys. 36 (1984) 219.
[58] J. Schwinger, J. Math. Phys. 2 (1961) 407.
[59] L. V. Keldysh, JETP 47 (1965) 1515.
[60] A. Kossakowski, Rep. Math. Phys. 3 (1972) 247.
[61] G. Lindblad, Commun. Math. Phys. 48 (1976) 119.
[62] K. Kraus, States, Effects and Operations, Fundamental Notions of Quantum Theory, Academic, Berlin (1983).
[63] H. G. Evertz, G. Lana, and M. Marcu, Phys. Rev. Lett. 70 (1993) 875.
[64] U.-J. Wiese and H.-P. Ying, Z. Phys. B93 (1994) 147.
[65] B. B. Beard and U.-J. Wiese, Phys. Rev. Lett. 77 (1996) 5130.
[66] P. C. Hohenberg and B. I. Halperin, Rev. Mod. Phys. 49 (1977) 436.
[67] A. W. Sandvik and H. G. Evertz, Phys. Rev. B82 (2010) 024407.
[68] U. Gerber, C. P. Hofmann, F.-J. Jiang, M. Nyfeler, and U.-J. Wiese, J. Stat. Mech. (2009) P03021.
[69] M. Nyfeler, F.-J. Jiang, F. Kämpfer, and U.-J. Wiese, Phys. Rev. Lett. 100 (2008) 247206.